Electronic Research Archive

https://www.aimspress.com/journal/era

ERA, 33(8): 5064–5084.
DOI: 10.3934/era.2025227
Received: 01 July 2025
Revised: 03 August 2025
Accepted: 20 August 2025
Published: 29 August 2025

Research article

Hopf bifurcation analysis of the delayed diffusive predator-prey model with harvesting terms

Honglu Yu[1], **Yu Sui**[1], **Dan Jin**[1,*] **and Ruizhi Yang**[1,2]

[1] Department of Mathematics, Northeast Forestry University, Harbin 150040, China
[2] School of Ecology, Northeast Forestry University, Harbin 150040, China

* **Correspondence:** Email: jindan720@163.com.

Abstract: This paper studied a delayed diffusive predator-prey model with predator and prey harvesting terms. The existence of constant steady-state solutions and Hopf bifurcation were analyzed. Then by applying the central manifold theorem and the normal form method, the direction of the Hopf bifurcation and stability of the bifurcating period solution were studied. Numerical simulations were conducted to confirm the accuracy of the proposed theory. In addition, taking the predator-prey relationship between sharks and tuna as an example, this study investigated the impact of predator harvesting coefficients on the constant steady-state solutions of the system and the time required for the system to reach stability.

Keywords: predator-prey model; delay; harvesting term; Hopf bifurcation

1. Introduction

The population dynamics of predator and prey within an ecosystem are shaped not just by their relative densities, but also by various environmental factors including resource availability, interspecific competition, and human harvesting activities. In the field of mathematical biology, predator-prey systems are widely used as important tools for describing and analyzing species interactions and population dynamics in ecosystems [1–4]. Researchers utilize this system to effectively depict the complex interactions between predator and prey, and subsequently describe population changes under different environmental conditions [5–7]. They study how these complex factors affect the stability and evolutionary trends of species populations, thus helping us gain a deeper understanding of the complexity of ecosystems [8–11].

In [1], the authors incorporated intraspecific cannibalism into the predator-prey model to account for competition-alleviating mechanisms under resource limitation. In [2], the authors conducted a systematic analysis of pattern formation dynamics in a harvested predator-prey system subject to

no-flux boundary conditions, revealing that the prey's diffusion rate determines the emergent spatial patterns. In [3], the authors proposed a predator-prey model incorporating prey refuge effects that are functionally dependent on predator size.

In [12], the authors proposed the following functional response:

$$\varphi(u, v) = \frac{Ce_0uv}{1 + hCe_0uv}.$$

The traditional Holling-type functional response [13] typically describes the change in the predation rate based on prey size, while this functional response simultaneously considers the effects of both prey size and predator size on the predation rate, reflecting the interactions between predators. K. Ryu et al. [14] studied the following system.

$$\begin{cases} \frac{du}{dt} = ru\left(1 - \frac{u}{K}\right) - \frac{Ce_0uv^2}{1+hCe_0uv}, \\ \frac{dv}{dt} = \frac{\epsilon Ce_0uv^2}{1+hCe_0uv} - \mu v. \end{cases} \tag{1.1}$$

u is the prey size. v is the predator size. The biological meanings and units of other parameters are presented in Table 1.

Table 1. Parameters descriptions and units in model (1.1).

Parameter	Description	Unit
u	Prey population density	$ind. \cdot m^{-2}$
v	Predator population density	$ind. \cdot m^{-2}$
r	Prey intrinsic growth rate	$year^{-1}$
C	Capture rate	$(ind. \cdot m^2)^{-1} \cdot year^{-1}$
h	Handling time	$year \cdot m^2 \cdot ind.^{-1}$
μ	Predator mortality rate	$year^{-1}$
K	Prey carrying capacity	$ind. \cdot m^{-2}$
e_0	Encounter rate	/
ϵ	Conversion efficiency	/

We use the following parameter transformations:

$$rt = \bar{t}, \ \ \frac{u}{K} = \bar{u}, \ \ hCe_0Ky = \bar{v}, \ \ \frac{1}{Ce_0(hK)^2r} = \alpha_1, \ \ \frac{\epsilon}{rh} = \alpha_2, \ \ \frac{\mu h}{\epsilon} = \gamma. \tag{1.2}$$

System (1.1) is turned to

$$\begin{cases} \frac{du}{dt} = u\,(1 - u) - \frac{\alpha_1uv^2}{1+uv}, \\ \frac{dv}{dt} = \alpha_2\left(\frac{uv^2}{1+uv} - \gamma v\right). \end{cases} \tag{1.3}$$

K. Ryu et al. [14] focused on the study of saddle points, Hopf bifurcation, and Bogdanov-Takens bifurcation in the context of coexistence constant steady-state solution states.

Since the survival struggle between predator and prey is affected by diffusion phenomena and energy conversion delays, the reactive diffusion term and time delay can more accurately reflect natural states.

In [15, 16], the authors examined the effects of the diffusion term and time delay on predator-prey models, studying the instability caused by time delay and the Hopf bifurcation at the positive constant steady-state solution.

Meanwhile, the survival of species in the real world is also affected by human intervention. In light of this, many researchers have carefully studied the impact of human influence on the predator-prey system [17–19], making it more aligned with real-life situations.

Inspired by their work, we expanded the spatial domain on the basis of [12] and focused on the effects of two harvesting terms on predator-prey models compared to [15, 17]. We further studied the following system, which builds on system (1.1) by considering the time delay between the predator consuming the prey and the birth of new individuals, as well as the diffusion and harvesting of both the predator and prey.

$$\begin{cases} \frac{\partial u(x,t)}{\partial t} = u(1-u) - \frac{\alpha_1 uv^2}{1+uv} - h_1 u + d_1 \Delta u, \quad x \in \Omega, t > 0, \\ \frac{\partial v(x,t)}{\partial t} = \frac{\alpha_2 u(t-\tau)v^2(t-\tau)}{1+u(t-\tau)v(t-\tau)} - (\gamma + h_2)v + d_2 \Delta v, \quad x \in \Omega, t > 0, \\ \frac{\partial u(x,t)}{\partial \nu} = \frac{\partial v(x,t)}{\partial \nu} = 0, \quad x \in \partial\Omega, t > 0, \\ u(x,t) = u_1(x,t) \geq 0, v(x,t) = v_1(x,t) \geq 0, \quad x \in \Omega, t \in [-\tau, 0]. \end{cases} \tag{1.4}$$

All parameters are positive. d_1 and d_2 are diffusion coefficients of the prey and predator, respectively. τ is the gestation delay. h_1 and h_2 are harvesting coefficients of the prey and predator, respectively. This type of model is widely observed in ecological systems. In marine ecosystems, many cartilaginous fish species prey on other fish. These organisms engage in activities such as metabolism, reproduction, and migration. They are captured by humans for various reasons. Therefore, their predator-prey dynamics can be modeled using reaction-diffusion equations with time delays. Similarly, this model is equally applicable to forest ecosystems where pests are controlled by their natural predators, as well as grassland systems where herbivorous animals like rabbits are hunted by predators such as wolves.

The rest of this paper is organized as follows. In Section 2, the stability of the coexisting constant steady-state solution and existence of Hopf bifurcation is studied. In Section 3, the property of Hopf bifurcation is studied. In Section 4, some numerical simulations are given. In Section 5, a short conclusion is given.

2. Stability analysis

Similar to the results in [14], it is straightforward to show that the existence of constant steady-state solutions for model (1.4).

Lemma 2.1. *The existence of constant steady-state solutions for model* (1.4) *can be broken down into four scenarios.*

1) $(0, 0)$ *and* $(1 - h_1, 0)$ *are two boundary equilibria of model* (1.4).

2) Model (1.4) *has no positive constant steady-state solution for* $\alpha_1 > \alpha_{\text{bt}} := \frac{4(1-h_1)^3\alpha_2(\alpha_2-\gamma-h_2)}{27(\gamma+h_2)^2}$.

3) Model (1.4) *has one positive constant steady-state solution* $(\frac{2}{3}(1 - h_1), \frac{3(\gamma+h_2)}{2(\alpha_2-\gamma-h_2)(1-h_1)})$ *for* $\alpha_1 = \alpha_{\text{bt}}$ *and* $\alpha_2 > \gamma + h_2$.

4) System (1.4) *has two distinct constant steady-state solutions* $(u_1,\ v_1)$ *and* $(u_2,\ v_2)$*, where* $u_1 < \frac{2}{3}(1 - h_1) < u_2$*, and* $u_{1,2}$ *are two roots of* $u^3 + (h_1 - 1)u^2 + \frac{\alpha_1(\gamma+h_2)^2}{\alpha_2(\alpha_2-\gamma-h_2)} = 0$*,* $v_{1,2} = \dfrac{\gamma + h_2}{(\alpha_2 - \gamma - h_2)u_{1,2}}$ *for* $\alpha_1 < \alpha_{\rm bt}$ *and* $\alpha_2 > \gamma + h_2$*.*

We make the following assumption:

$$(\mathbf{H_0}) \qquad \alpha_1 \le \alpha_{bt}, \quad \gamma + h_2 < \alpha_2.$$

If $(\mathbf{H_0})$ holds, model (1.4) has one or two constant steady-state solutions. We represent $E_*(u_*, v_*)$ as coexisting constant steady-state solutions and linearize system (1.4) at $E_*(u_*, v_*)$:

$$\frac{\partial u}{\partial t}\begin{pmatrix} u(x,t) \\ u(x,t) \end{pmatrix} = D\begin{pmatrix} \Delta u(t) \\ \Delta v(t) \end{pmatrix} + L_1\begin{pmatrix} u(x,t) \\ v(x,t) \end{pmatrix} + L_2\begin{pmatrix} u(x,t-\tau) \\ v(x,t-\tau) \end{pmatrix}, \tag{2.1}$$

where

$$D = \begin{pmatrix} d_1 & 0 \\ 0 & d_2 \end{pmatrix}, \quad L_1 = \begin{pmatrix} a_1 & a_2 \\ 0 & -\gamma - h_2 \end{pmatrix}, \quad L_2 = \begin{pmatrix} 0 & 0 \\ b_1 & b_2 \end{pmatrix},$$

and $a_1 = \frac{u_* v_*^3 \alpha_1}{(1+u_* v_*)^2} - u_*$, $a_2 = -\frac{u_* v_* (2+u_* v_*)\alpha_1}{(1+u_* v_*)^2} < 0$, $b_1 = \frac{v_*^2 \alpha_2}{(1+u_* v_*)^2} > 0$, $b_2 = \frac{u_* v_* (2+u_* v_*)\alpha_2}{(1+u_* v_*)^2} > 0$.

We obtain

$$\lambda^2 + A_1\lambda + A_2 + (A_3 - b_2\lambda)e^{-\lambda\tau} = 0, \ \ k \in \mathbb{N}_0, \tag{2.2}$$

where

$$\begin{aligned} &A_1 = (d_1 + d_2)\frac{k^2}{l^2} + (\gamma + h_2) - a_1, \ \ A_2 = d_1 d_2 \frac{k^4}{l^4} + [(\gamma + h_2)d_1 - a_1 d_2]\frac{k^2}{l^2} - a_1(\gamma + h_2), \\ &A_3 = -b_2 d_1 \frac{k^2}{l^2} + a_1 b_2 - a_2 b_1, \ \ k \in \mathbb{N}_0. \end{aligned} \tag{2.3}$$

2.1. The situation of $\tau = 0$

When $\tau = 0$, (2.2) is

$$\lambda^2 + (A_1 - b_2)\lambda + A_2 + A_3 = 0, \quad k \in \mathbb{N}_0. \tag{2.4}$$

We make the following assumption:

$$(\mathbf{H_1}) \qquad A_1 - b_2 > 0,\ A_2 + A_3 > 0, \text{ for } k \in \mathbb{N}_0.$$

Theorem 2.1. *For model* (1.4)*, if* $(\mathbf{H_0})$ *and* $(\mathbf{H_1})$ *hold,* $E_*(u_*, v_*)$ *is locally asymptotically stable when* $\tau = 0$*.*

Proof. If $(\mathbf{H_1})$ is set, it follows that the eigenvalues of (2.4) all have a negative real radical.

2.2. The situation of $\tau > 0$

When $\tau > 0$, let $\mathrm{i}\omega$ $(\omega > 0)$ be a solution of (2.2). Then

$$-\omega^2 + \mathrm{i}\omega A_1 + A_2 + (A_3 - b_2\mathrm{i}\omega)(\cos\omega\tau - \mathrm{i}\sin\omega\tau) = 0.$$

We can obtain

$$\begin{cases} -w^2 + A_2 + A_3\cos\omega\tau - wb_2\sin\omega\tau = 0, \\ A_1 w - A_3\sin\omega\tau - wb_2\cos\omega\tau = 0. \end{cases}$$

This leads to $\cos\omega\tau = \frac{\omega^2(b_2A_1+A_3)-A_2A_3}{A_3^2+b_2^2\omega^2}$, $\sin\omega\tau = \frac{\omega\left(A_1A_3+A_2b_2-b_2\omega^2\right)}{A_3^2+b_2^2\omega^2}$.
In addition,

$$\omega^4 + \omega^2\left(A_1^2 - 2A_2 - b_2^2\right) + A_2^2 - A_3^2 = 0. \tag{2.5}$$

Let $m = \omega^2$, and then (2.5) becomes

$$m^2 + m\left(A_1^2 - 2A_2 - b_2^2\right) + A_2^2 - A_3^2 = 0, \tag{2.6}$$

and the roots of (2.6) are $m^{\pm} = \frac{1}{2}[-F_k \pm \sqrt{F_k^2 - 4G_kR_k}]$, where $F_k = A_1^2 - 2A_2 - b_2^2$, $G_k = A_2 + A_3$, and $R_k = A_2 - A_3$. If $(\mathbf{H_0})$ and $(\mathbf{H_1})$ hold, $G_k > 0$ $(k \in \mathbb{N}_0)$. We have

$$\begin{aligned} F_k &= \left(h_2 + \gamma - a_1 + (d_1 + d2)\frac{k^2}{l^2}\right)^2 + 2\left(\frac{d_1d_2k^4}{l^4} - a_1(h_2+\gamma) + \frac{k^2(-a_1d_2 + d_1(h_2+\gamma))}{l^2}\right) - b_2^2, \\ R_k &= d_1d_2\frac{k^4}{l^4} + [b_2d_1 - a_1d_2 + d_1(\gamma + h_2)]\frac{k^2}{l^2} + a_2b_1 - a_1b_2 - a_1(\gamma + h_2) \quad \text{for } k \in \mathbb{N}_0. \end{aligned}$$

Define

$$\begin{aligned} \mathbb{S}_1 &= \{k | R_k < 0,\ k \in \mathbb{N}_0\}, \\ \mathbb{S}_2 &= \{k | R_k > 0,\ F_k < 0,\ F_k^2 - 4G_kR_k > 0,\ k \in \mathbb{N}_0\}, \\ \mathbb{S}_3 &= \{k | R_k > 0,\ F_k^2 - 4G_kR_k < 0,\ k \in \mathbb{N}_0\}, \end{aligned}$$

and

$$\begin{aligned} \omega_k^{\pm} &= \sqrt{m_k^{\pm}}, \quad \tau_k^{j,\pm} = \begin{cases} \frac{1}{\omega_k^{\pm}}\arccos(V_{cos}^{(k,\pm)}) + 2j\pi, & V_{sin}^{(k,\pm)} \geq 0, \\ \frac{1}{\omega_k^{\pm}}\left[2\pi - \arccos(V_{cos}^{(k,\pm)})\right] + 2j\pi, & V_{sin}^{(k,\pm)} < 0, \end{cases} \\ V_{cos}^{(k,\pm)} &= \frac{(\omega_k^{\pm})^2(b_2A_1 + A_3) - A_2A_3}{A_3^2 + b_2^2(\omega_k^{\pm})^2}, \ V_{sin}^{(k,\pm)} = \frac{\omega_k^{\pm}\left(A_1A_3 + A_2b_2 - b_2(\omega_k^{\pm})^2\right)}{A_3^2 + b_2^2(\omega_k^{\pm})^2}. \end{aligned} \tag{2.7}$$

Lemma 2.2. *When* $(\mathbf{H_0})$ *and* $(\mathbf{H_1})$ *hold, the roots of* (2.2) *can be classified into three cases.*

1) $k \in \mathbb{S}_1$*: a pair of purely imaginary roots* $\pm i\omega_k^+$ *at* $\tau_k^{j,+}$ *for* $j \in \mathbb{N}_0$.

2) $k \in \mathbb{S}_2$*: two pairs of purely imaginary roots* $\pm i\omega_k^{\pm}$ *at* $\tau_k^{j,\pm}$ *for* $j \in \mathbb{N}_0$.

3) $k \in \mathbb{S}_3$*: no purely imaginary root.*

Proof. When $k \in \mathbb{S}_1$, m^+ is the positive real root, m^- is the negative real root. Then we can obtain case 1). When $k \in \mathbb{S}_2$, $m_k^{\pm}$ are two positive real roots. Then we can obtain case 2). When $k \in \mathbb{S}_3$, $m_k^{\pm}$ are two negative real roots. Then we can obtain case 3).

Lemma 2.3. *Assume* $(\mathbf{H_0})$ *and* $(\mathbf{H_1})$ *hold, and then* $Re(\frac{d\lambda}{d\tau})|_{\tau=\tau_k^{j,+}} > 0$, $Re(\frac{d\lambda}{d\tau})|_{\tau=\tau_k^{j,-}} < 0$ *for* $k \in \mathbb{S}_1 \cup \mathbb{S}_2$ *and* $j \in \mathbb{N}_0$.

Proof. By (2.2), we have

$$(\frac{d\lambda}{d\tau})^{-1} = \frac{2\lambda + A_1 - b_2 e^{-\lambda\tau}}{(A_3 - b_2\lambda)\lambda e^{-\lambda\tau}} - \frac{\tau}{\lambda}.$$

Then

$$\begin{aligned}[\mathrm{Re}(\frac{d\lambda}{d\tau})^{-1}]_{\tau=\tau_k^{j,\pm}} &= \mathrm{Re}[\frac{2\lambda + A_1 - b_2 e^{-\lambda\tau}}{(A_3 - b_2\lambda)\lambda e^{-\lambda\tau}} - \frac{\tau}{\lambda}]_{\tau=\tau_k^{j,\pm}} \\ &= [\frac{1}{A_3^2 + b_2^2\omega^2}(2\omega^2 + A_1^2 - 2A_2 - b_2^2)]_{\tau=\tau_k^{j,\pm}} \\ &= \pm[\frac{1}{A_3^2 + b_2^2\omega^2}\sqrt{(A_1^2 - 2A_2 - b_2^2)^2 - 4(A_2^2 - A_3^2)}]_{\tau=\tau_k^{j,\pm}}.\end{aligned}$$

Therefore $\mathrm{Re}(\frac{d\lambda}{d\tau})|_{\tau=\tau_k^{j,+}} > 0$, $\mathrm{Re}(\frac{d\lambda}{d\tau})|_{\tau=\tau_k^{j,-}} < 0$.

Denote $\tau_* = min\{\tau_k^0 |\ k \in \mathbb{S}_1 \cup \mathbb{S}_2\}$. We can obtain the following theorem.

Theorem 2.2. *When* ($\mathbf{H_0}$) *and* ($\mathbf{H_1}$) *hold, model* (1.4) *has four situations.*

1) If $\mathbb{S}_1 \cup \mathbb{S}_2 = \varnothing$, $E_*(u_*, v_*)$ *is locally asymptotically stable for* $\tau > 0$.

2) If $\mathbb{S}_1 \cup \mathbb{S}_2 \neq \varnothing$, $E_*(u_*, v_*)$ *is locally asymptotically stable for* $\tau \in [0, \tau_*)$.

3) If $\mathbb{S}_1 \cup \mathbb{S}_2 \neq \varnothing$, $E_*(u_*, v_*)$ *is unstable for* $\tau \in (\tau_*, \tau_* + \varepsilon)$ *for some* $\varepsilon > 0$.

4) Hopf bifurcation occurs at $E(u_*, v_*)$ *when* $\tau = \tau_k^{j,+}$ ($\tau = \tau_k^{j,-}$), $j \in \mathbb{N}_0$, *and* $k \in \mathbb{S}_1 \cup \mathbb{S}_2$.

3. Properties of Hopf bifurcation

Here we define

$$\begin{aligned}c_1(0) &= \frac{i}{2\omega_k\dot{\tau}}\left(g_{20}g_{11} - 2|g_{11}|^2 - \frac{|g_{02}|^2}{3}\right) + \frac{1}{2}g_{21}, \\ \xi_2 &= -\frac{\mathrm{Re}(c_1(0))}{\mathrm{Re}(\lambda'(\tau_k^j))}, \\ T_2 &= -\frac{1}{\omega_k\dot{\tau}}[\mathrm{Im}(c_1(0)) + \xi_2\mathrm{Im}(\lambda'(\tau_k^j))], \\ \beta_2 &= 2\mathrm{Re}(c_1(0)),\end{aligned}$$

where

$$g_{20} = \gamma_1\dot{\tau}\chi_{20} + \gamma_2\dot{\tau}\varsigma_{20}, \quad g_{11} = \gamma_1\dot{\tau}\chi_{11} + \gamma_2\dot{\tau}\varsigma_{11}, \quad g_{02} = \gamma_1\dot{\tau}\overline{\chi}_{20} + \gamma_2\dot{\tau}\overline{\varsigma}_{20}, \tag{3.1}$$

and for $k \in \mathbb{N}_0$, we have $g_{21} = \dot{\tau}(\gamma_1\kappa_1 + \gamma_2\kappa_2)$. The detailed computation is given in the Appendix of the works [20, 21].

Theorem 3.1. *For the model* (1.4), *assume* (H_0) *and* (H_1) *hold. For any critical value* τ_k^{j+} *(or* τ_k^{j-}*), the bifurcating periodic solutions exist for* $\tau > \tau_k^{j+}$ *(or* $\tau < \tau_k^{j-}$*) when* $\xi_2 > 0$ *(or* $\xi_2 < 0$*) and are orbitally asymptotically stable (or unstable) when* $\beta_2 < 0$ *(or* $\beta_2 > 0$*).*

4. Numerical simulations

We present numerical simulations of model (1.4) to examine the effects of delays and harvesting terms. The parameters are selected as shown in Table 2.

Table 2. Parameter - Value Table.

Parameter	Value	Parameter	Value
α_1	0.05	α_2	1.748
h_1	0.1	h_2	0.9
d_1	0.3	d_2	0.2
γ	0.4	l	2

At this time, we have two positive equilibria $E_1 \approx (0.589608, 4.92155)$ and $E_2 \approx (0.610273, 4.7549)$ that satisfy H_0. Since E_2 is unstable, we mainly analyze the property of the model (1.4) at E_1. Through direct calculation, we obtain $A_1 \approx 1.65877$, $b_2 \approx 1.63318$, $A_2 \approx 0.466398$, and $A_3 \approx -0.456011$ for k=0 . Then $A_1 - b_2 > 0$ and $A_2 + A_3 > 0$, which satisfy H_1. $\omega_0 \approx 0.914943$, $\tau_* = \tau_0^0 \approx 6.28172$. From Theorem 2.2, we know that a Hopf bifurcation occurs at $\tau = \tau_*$. From Theorem 3.1, $\mu_2 \approx 1908.34 > 0$, $\beta_2 \approx -22.904 < 0$, and $T_2 \approx 36.0408 > 0$.

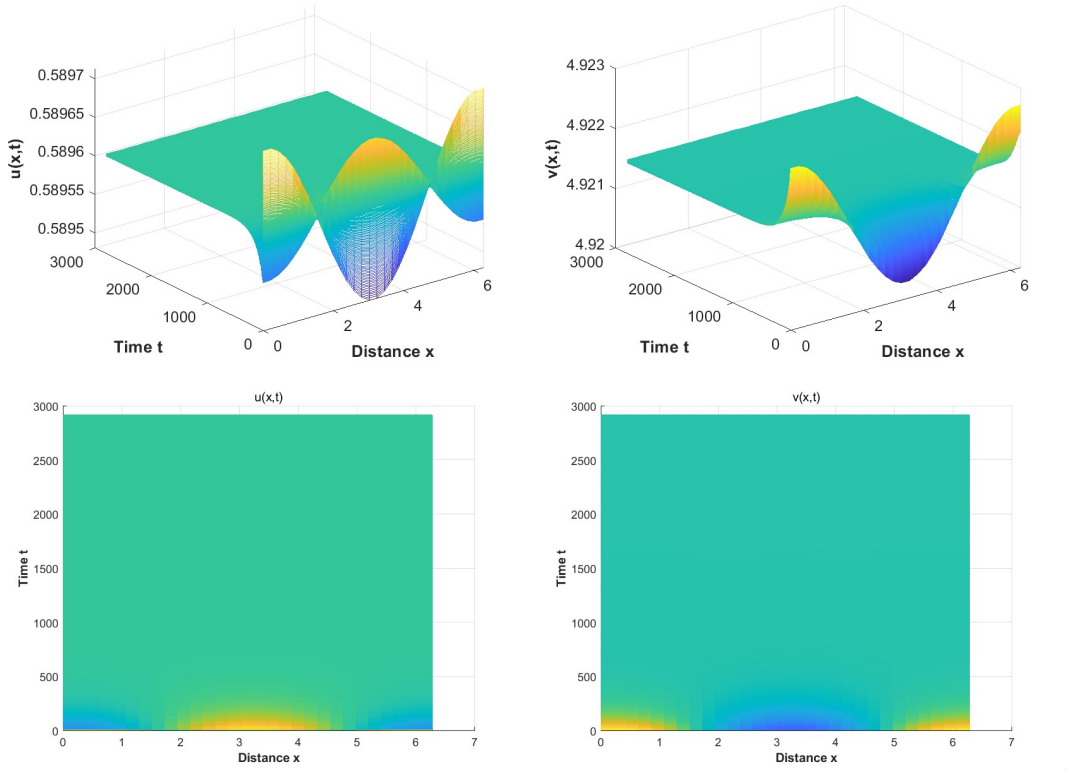

Figure 1. When $\tau = 6.2 < \tau_0^0$ and the other parameters are the same as shown in Table 2, we show the simulated solutions for the size of the prey (left) and the size of the predator (right), where the system is locally asymptotically stable.

From Theorem 2.2, E_1 is locally asymptotically stable for $\tau \in [0, \tau_*)$, which can be shown in Figure 1, where we choose $\tau = 6.2$. This indicates that when the gestation delay of the predator is lower than the critical value, the system eventually stabilizes. Stably spatially inhomogeneous bifurcating periodic solutions exist for $\tau > \tau_*$, and there exist stable spatially inhomogeneous bifurcating periodic solutions. This is shown in Figure 2, where we choose $\tau = 6.3$. This indicates that when the predator's gestation period exceeds the critical value, the system exhibits periodic behavior. This mechanistic framework explains the periodic oscillations observed between cartilaginous fish species such as sharks and their prey populations in marine ecosystems, while offering enhanced theoretical justification for implementing ecosystem-based fishery management strategies, with particular relevance to fishing cycle regulation.

Next, we keep the values of other parameters unchanged and vary the harvest term coefficients h_1 and h_2 to study their influence on model (1.4).

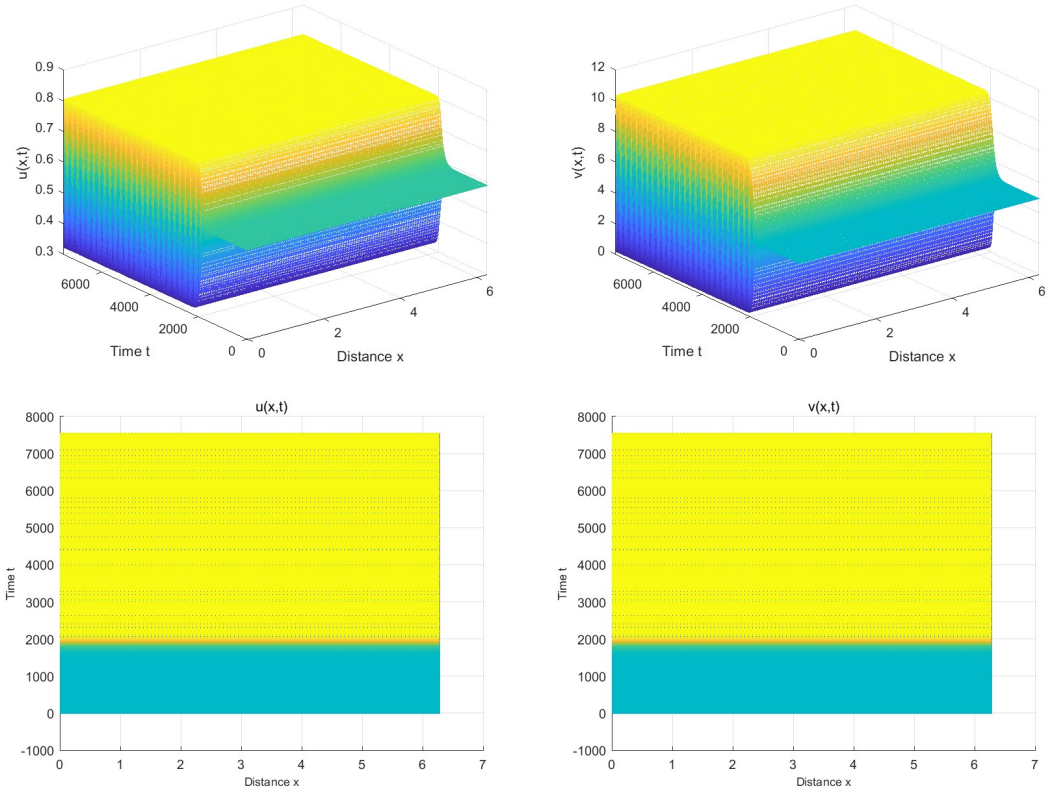

Figure 2. When $\tau = 6.3 > \tau_0^0$ and the other parameters are the same as shown in Table 2, we show the simulated solutions for the size of the prey (left) and the size of the predator (right), where the system is periodic.

Here, we fix $h_2 = 0.9$ and vary h_1 from 0 to 0.1. At this point we find that τ is always less than τ_0^0 and therefore convergent. In this case, the third case of Lemma 2.1, meaning there are two constant steady-state solutions, we use MATLAB to plot the changes in the constant steady-state solutions of the predator and prey with respect to h_1, which is shown in Figure 3. Under the assumption that other factors are not considered, as the harvest amount of prey increases, the prey size at the larger

constant steady-state solution (dashed line) decreases. Here, the predator size (dashed line) increases. Meanwhile, the prey size at the smaller constant steady-state solution (solid line) increases while the predator size (solid line) decreases. The density changes of the predator and prey at the other constant steady-state solution follow an opposite trend. Eventually, the two constant steady-state solutions tend to be equal.

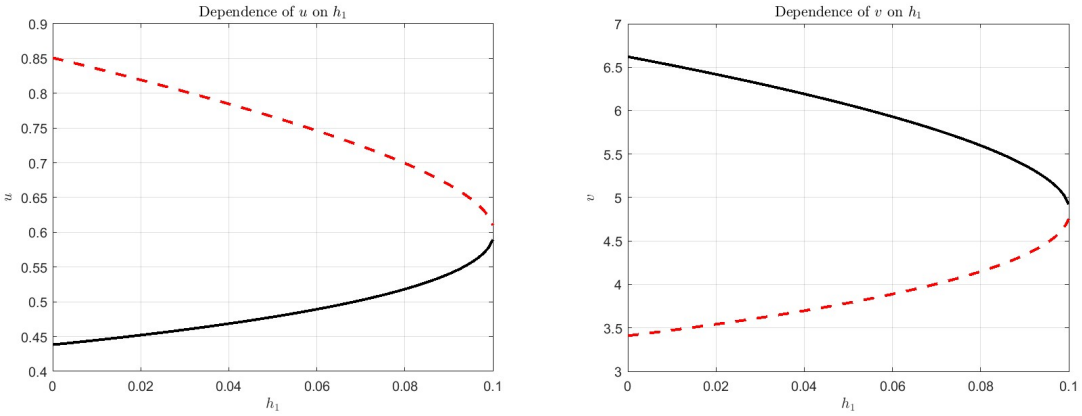

Figure 3. Changes in the two constant steady-state solutions of prey size (left) and predator size (right) with prey harvest h_1. The other parameters are the same as shown in Table 2.

Next, we fix $h_1 = 0.1$ and vary h_2 from 0 to 0.9. At this point we find that τ is always less than τ_0^0 and therefore convergent. Under these conditions, system (1.4) also has two constant steady-state solutions, as shown in Figure 4. Under the assumption that other factors are not considered, as the predator harvest increases, the prey size at the larger constant steady-state solution (dashed line) decreases, while the predator size (dashed line) increases. Meanwhile, the prey size at the smaller constant steady-state solution (solid line) increases. It is worth noting that the predator size (solid line) first increases and then decreases, with the inflection point referred to as the maximum capture point. Eventually, the two constant steady-state solutions tend to become equal.

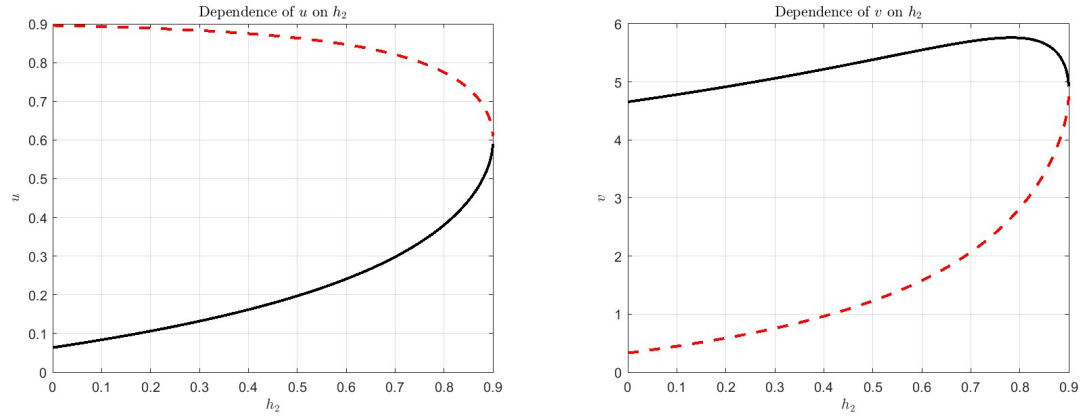

Figure 4. Changes in the two constant steady-state solutions of prey size (left) and predator size (right) with predator harvest h_2. The other parameters are the same as shown in Table 2.

We also investigated the effect of harvesting terms on the critical τ.

Here we keep other parameters constant and setting $h_2 = 0.9$, then:

If $h_1 < 0.099$, $\mathbf{H_1}$ is not satisfied, implying no critical τ exists.

If $h_1 > 0.1$, $\mathbf{H_0}$ is not satisfied, indicating no positive constant steady-state solution exists.

When h_1 is in [0.099, 0.1], the critical τ increases with the increase of prey harvesting h_1.

Here we keep other parameters constant and setting $h_1 = 0.1$, then:

If $h_2 < 0.899$, $\mathbf{H_1}$ is not satisfied, meaning no critical τ exists.

If $h_2 > 0.9$, $\mathbf{H_0}$ is not satisfied, indicating no positive constant steady-state solution exists.

When h_2 is in [0.899, 0.9], the critical τ increases with the increase of predator harvesting h_2.

Additionally, we study the impact of the harvesting term on the time it takes for the system to reach stability. Here we specify that the fluctuation range of the prey population u is considered to be in a stable state when the range of u dose not exceed 10^{-6}. Taking $h_2 = 0.9$, we use MATLAB to plot the time for system (1.4) to reach stability when h_1 takes 0.099, 0.0995, and 0.1, which is shown in Figure 5. From the figure, the time for the prey to reach stability increases with the increase in prey harvesting h_1.

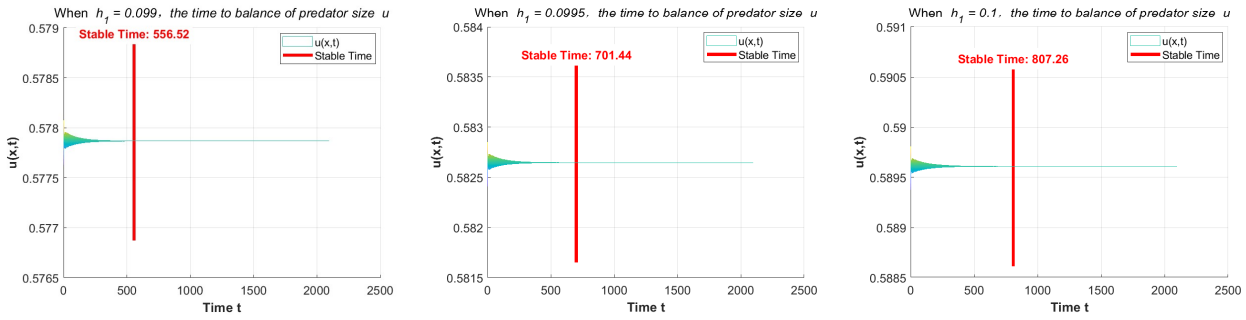

Figure 5. The time chart of the system reaching stability when taking different values of h_1.

In Figure 4, it is observed that when other parameters remain unchanged and $h_1 = 0.1$, the predator size at the constant steady-state solution will have an inflection point as h_2 changes. Further research shows that values of h_2 smaller than the inflection point part will make the system not satisfy ($\mathbf{H_0}$). Therefore, we keep $h_1 = 0.1$ unchanged and plot the time for system (1.4) to reach stability when h_2 takes 0.899, 0.8995, and 0.9, which is shown in Figure 6. Here we specify that the fluctuation range of the predator size is considered to be in a stable state when the range of v dose not exceed 10^{-6}. It is clear from the figure that the time for the system to reach stability increases with the increase in predator harvesting h_2.

Increased human fishing directly reduces the tuna population, leading to a shortage of food resources for predatory sharks. Due to reproductive time lags, sharks cannot rapidly compensate for prey decline through population growth, delaying the recovery of their prey-regulation capacity. Consequently, rebuilding predator-prey dynamic equilibrium requires more time, ultimately prolonging the system's recovery period. This demonstrates how biological reproductive delays and fishing activities jointly affect ecosystem stability.

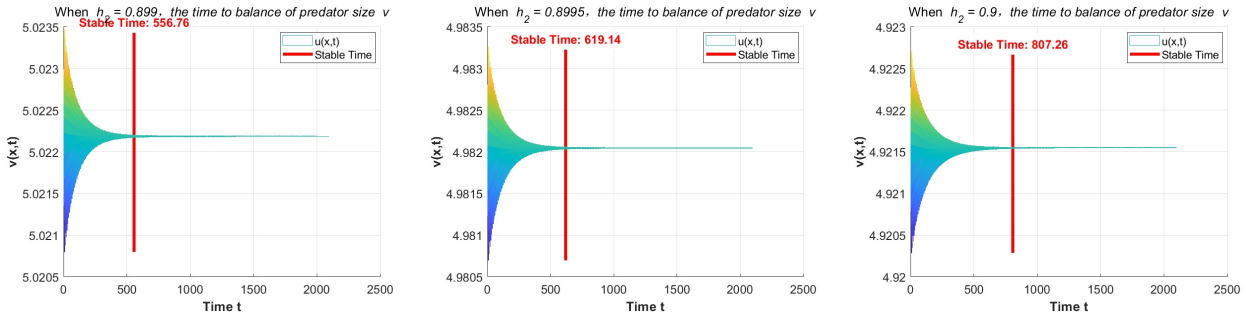

Figure 6. The time chart of the system reaching stability when taking different values of h_2.

5. Conclusions

In this paper, we analyze a diffusion predator-prey system with predator and prey harvesting terms and gestation delay, and study the impact of time delay and harvesting terms on the system's dynamic behavior. We study the stability of the coexistence constant steady-state solution and the existence of Hopf bifurcation. Using the center manifold theorem and normal form method, we investigate the properties of the Hopf bifurcation. Numerical simulations are conducted to validate the theoretical results. Our findings show that when the predator's gestation period is below the critical value, the system tends to stabilize. However, when the gestation period exceeds this critical value, the system exhibits periodic behavior. In ecology, this explains the shift in population dynamics from stable equilibrium to periodic oscillations. As for the harvesting term, it not only affects the system's constant steady-state solution but also influences the time required for the system to reach stability. This study investigates the effects of reproductive time delays and harvesting terms on population dynamics, using sharks and tuna in marine ecosystems as a representative case study.

Author Contributions

The idea of this research was introduced by H. Yu and D. Jin. All authors contributed to the main results and numerical simulations.

Use of AI tools declaration

The authors declare they have not used Artificial Intelligence (AI) tools in the creation of this article.

Acknowledgments

This research is supported by the Northeast Forestry University College Student Innovation and Entrepreneurship Training Program Project (No. DCLXY-2025015).

Conflict of interest

The authors declare there is no conflict of interest.

References

1. D. F. Duan, B. Niu, J. Wei, Y. Yuan, The dynamical analysis of a nonlocal predator-prey model with cannibalism, *Eur. J. Appl. Math.*, **35** (2025), 707–731. https://doi.org/10.1017/S0956792524000019
2. M. Chen, S. Ham, Y. Choi, H. Kim, J. Kim, Pattern dynamics of a harvested predator-prey model, *Chaos, Solitons Fractals*, **176** (2023), 114153. https://doi.org/10.1016/j.chaos.2023.114153
3. W. Yang, M. Chen, The impact of predator-dependent prey refuge on the dynamics of a leslie-Gower predator-prey model, *Asian Res. J. Math.*, **19** (2023), 203–211. https://doi.org/10.9734/arjom/2023/v19i11766
4. G. Guo, X. Yang, C. Zhang, S. Li, Pattern formation with jump discontinuity in a predator-prey model with Holling-II functional response, *Eur. J. Appl. Math.*, (2025), 1–23. https://doi.org/10.1017/S0956792525000063
5. F. Zhu, R. Yang, Bifurcation in a modified Leslie-Gower model with nonlocal competition and fear effect, *Discrete Contin. Dyn. Syst. - Ser. B*, **30** (2025), 2865–2893. https://doi.org/10.3934/dcdsb.2024195
6. F. Wang, R. Yang, X. Zhang, Turing patterns in a predator-prey model with double Allee effect, *Math. Comput. Simul.*, **220** (2024), 170–191. https://doi.org/10.1016/j.matcom.2024.01.015
7. R. Yang, F. Wang, D. Jin, Spatially inhomogeneous bifurcating periodic solutions induced by nonlocal competition in a predator-prey system with additional food, *Math. Methods Appl. Sci.*, **45** (2022), 9967–9978. https://doi.org/10.1002/mma.8349
8. P. A. Schmidt, L. D. Mech, Wolf pack size and food acquisition, *Am. Nat.*, **150** (1997), 513–517. https://doi.org/10.1086/286079
9. F. Courchamp, D. Macdonald, Crucial importance of pack size in the African wild dog Lycaon pictus, *Anim. Conserv.*, **4** (2010), 169–174. https://doi.org/10.1017/S1367943001001196
10. D. Scheel, C. Packer, Group hunting behaviour of lions: a search for cooperation, *Anim. Behav.*, **41** (1991), 697–709. https://doi.org/10.1016/S0003-3472(05)80907-8
11. Y. Ma, R. Yang, Bifurcation analysis in a modified Leslie-Gower with nonlocal competition and Beddington-DeAngelis functional response, *J. Appl. Anal. Comput.*, **15** (2025), 2152–2184. https://doi.org/10.11948/20240415
12. C. Cosner, D. L. Deangelis, J. S. Ault, D. B. Olson, Effects of spatial grouping on the functional response of predators, *Theor. Popul. Biol.*, **56** (1999), 65–75. https://doi.org/10.1006/tpbi.1999.1414
13. C. S. Holling, The functional response of predators to prey size and its role in mimicry and population regulation, *Mem. Entomol. Soc. Can.*, **97** (1965), 5–60. https://doi.org/10.4039/entm9745fv
14. K. Ryu, W. Ko, M. Haque, Bifurcation analysis in a predator-prey system with a functional response increasing in both predator and prey densities, *Nonlinear Dyn.*, **94** (2018), 1639–1656. https://doi.org/10.1007/s11071-018-4446-0
15. R. Yang, C. Nie, D. Jin, Spatiotemporal dynamics induced by nonlocal competition in a diffusive predator-prey system with habitat complexity, *Nonlinear Dyn.*, **110** (2022), 879–900. https://doi.org/10.1007/s11071-022-07625-x

16. X. Zhang, J. Liu, G. Wang, Impacts of nonlocal fear effect and delay on a reaction-diffusion predator-prey model, *Int. J. Biomath.*, **18** (2025), 2350089. https://doi.org/10.1142/S1793524523500894

17. X. Zhang, S. Li, Y. Yuan, Q. An, Effect of discontinuous harvesting on a diffusive predator-prey model, *Nonlinearity*, **37** (2024), 115016. https://doi.org/10.1088/1361-6544/ad7fc3

18. Y. Wang, Q. Tu, Multiple positive periodic solutions for a delayed predator-prey system with Beddington-DeAngelis functional response and harvesting terms, in *Annals of the University of Craiova, Mathematics and Computer Science Series*, **42** (2015), 330–338. https://doi.org/10.52846/ami.v42i2.644

19. X. Chang, J. Wei, Hopf bifurcation and optimal control in a diffusive predator-prey system with time delay and prey harvesting, *Nonlinear Anal.-Model. Control*, **17** (2012), 379–409. https://doi.org/10.15388/NA.17.4.14046

20. J. Wu, *Theory and Applications of Partial Functional Differential Equations*, Springer Berlin, 1996.

21. B. D. Hassard, N. D. Kazarinoff, Y. H. Wan, *Theory and Applications of Hopf Bifurcation*, Cambridge University Press, Cambridge-New York, 1981.

Appendix

A computation of normal form

Here, we give the following results by the method of [20, 21]. Let $\bar{u}(x,t) = u(x,\tau t) - u_*$ and $\bar{v}(x,t) = v(x,\tau t) - v_*$. For $j \in \mathbb{N}_0$ and $k \in \mathbb{S}_1 \cup \mathbb{S}_2$, we denote $\dot{\tau} = \tau_k^{j,\pm}$. Dropping the bar, (1.4) can be written as

$$\begin{cases} \dfrac{\partial u}{\partial t} = \tau[d_1\Delta u + (u+u_*)\,(1-(u+u_*)) - \dfrac{\alpha_1(u+u_*)(v+v_*)^2}{1+(u+u_*)(v+v_*)} - h_1(u+u_*)], \\ \dfrac{\partial v}{\partial t} = \tau[d_2\Delta v + \dfrac{\alpha_2(u(t-1)+u_*)(v(t-1)+v_*)^2}{1+(u(t-1)+u_*)(v(t-1)+v_*)} - (\gamma+h_2)(v+v_*)]. \end{cases} \tag{A.1}$$

Define $\tau = \dot{\tau} + \xi$, and B(t) $= (u(x,t), v(x,t))^T$, and we obtain

$$\frac{dB(t)}{dt} = \dot{\tau}D\Delta B(t) + L_{\dot{\tau}}(B_t) + Y(B_t,\xi), \tag{A.2}$$

where

$$L_\xi(\zeta) = \xi\begin{pmatrix} a_1\zeta_1(0) - a_2\zeta_2(0) \\ (\gamma+h_2)\zeta_2(0) + \ b_1\zeta_1(-1) + \ b_2\zeta_2(-1) \end{pmatrix} \tag{A.3}$$

and

$$Y(\zeta,\xi) = \xi D\Delta\zeta + L_\xi(\zeta) + y(\zeta,\xi), \tag{A.4}$$

with

$$y(\zeta,\xi) = (\dot{\tau}+\xi)(y_1(\zeta,\xi), y_2(\zeta,\xi))^T,$$

$$y_1(\zeta,\xi) = (\zeta_1(0)+u_*)\left(1-\zeta_1(0)-u_*-\frac{\alpha_1(\zeta_2(0)+v_*)^2}{1+(\zeta_1(0)+u_*)(\zeta_2(0)+u_*)}\right)-a_1\zeta_1(0)-a_2\zeta_2(0),$$

$$y_2(\zeta,\xi) = \alpha_2(\zeta_2(-1)+v_*)\left(\frac{(\zeta_1(-1)+u_*)(\zeta_2(-1)+v_*)}{1+(\zeta_1(-1)+u_*)(\zeta_2(-1)+v_*)}-\gamma-h_2\right)+(\gamma+h_2)\zeta_2(0)-b_1\zeta_1(-1)-b_2\zeta_2(-1),$$

respectively, for $\zeta=(\zeta_1,\zeta_2)^T\in C_1$.

Consider equation

$$\frac{dB(t)}{dt} = \dot\tau D\Delta B(t) + L_{\dot\tau}(B_t). \tag{A.5}$$

We know that $\Lambda_k := \{i\omega_k\dot\tau, -i\omega_k\dot\tau\}$ are characteristic roots of

$$\frac{dm(t)}{dt} = -i\dot\tau D\frac{k^2}{l^2}m(t) + L_{\dot\tau}(m_t). \tag{A.6}$$

Choose

$$\eta^n(\sigma,\tau) = \begin{cases}\tau E, & \sigma=0,\\ 0, & \sigma\in(-1,0),\\ -\tau Y, & \sigma=-1,\end{cases} \tag{A.7}$$

where

$$E=\begin{pmatrix}a_1-d_1\frac{k^2}{l^2} & a_2\\ 0 & -\gamma-h_2-d_2\frac{k^2}{l^2}\end{pmatrix},\quad Y=\begin{pmatrix}0&0\\ b_1&b_2\end{pmatrix}. \tag{A.8}$$

Define the bilinear paring

$$\begin{aligned}(\psi,\varphi) &= \psi(0)\varphi(0)-\int_{-1}^{0}\int_{\xi=0}^{s}\psi(\xi-s)d\eta^n(s,\tau)\varphi(\xi)d\xi\\ &= \psi(0)\varphi(0)+\dot\tau\int_{-1}^{0}\psi(\xi+1)Y\varphi(\xi)d\xi\end{aligned} \tag{A.9}$$

for $\varphi\in C([-1,0],\mathbb{R}^2)$ and $\psi\in C([0,1],\mathbb{R}^2)$. $\pm i\omega_k\dot\tau$ are eigenvalues of $A(\dot\tau)$, which are also eigenvalues of A^*. Define $p_1(\sigma)=(1,\delta)^Te^{i\omega_k\dot\tau s}(s\in[-1,0])$ and $q_1(r)=(1,\nu)e^{-i\omega_k\dot\tau r}(r\in[0,1])$, where

$$\delta=\frac{1}{a_2}\left(-a_1+d_1\frac{n^2}{l^2}+i\omega_k\right),\quad \nu=-\frac{e^{-i\dot\tau\omega_k}}{b_1}\left(a_1-d_1\frac{n^2}{l^2}+i\omega_k\right).$$

Let $\Phi=(\Phi_1,\Phi_2)$ and $\Upsilon^*=(\Upsilon_1^*,\Upsilon_2^*)^T$ with

$$\Phi_1(s)=\frac{p_1(s)+p_2(s)}{2}=\begin{pmatrix}\mathrm{Re}(e^{i\omega_k\dot\tau s})\\ \mathrm{Re}(\delta e^{i\omega_k\dot\tau s})\end{pmatrix},\quad \Phi_2(s)=\frac{p_1(s)-p_2(s)}{2i}=\begin{pmatrix}\mathrm{Im}(e^{i\omega_k\dot\tau s})\\ \mathrm{Im}(\delta e^{i\omega_k\dot\tau s})\end{pmatrix}$$

for $\sigma\in[-1,0]$ and

$$\Upsilon_1^*(r)=\frac{q_1(r)+q_2(r)}{2}=\begin{pmatrix}\mathrm{Re}(e^{-i\omega_k\dot\tau r})\\ \mathrm{Re}(\nu e^{-i\omega_k\dot\tau r})\end{pmatrix},\quad \Upsilon_2^*(r)=\frac{q_1(r)-q_2(r)}{2i}=\begin{pmatrix}\mathrm{Im}(e^{-i\omega_k\dot\tau r})\\ \mathrm{Im}(\nu e^{-i\omega_k\dot\tau r})\end{pmatrix}$$

for $r\in[0,1]$. Then by (4.8) we obtain

$$D_1^*:=(\Upsilon_1^*,\Phi_1),\quad D_2^*:=(\Upsilon_1^*,\Phi_2),\quad D_3^*:=(\Upsilon_2^*,\Phi_1),\quad D_4^*:=(\Upsilon_2^*,\Phi_2).$$

Define $(\Upsilon^*, \Phi) = (\Upsilon_j^*, \Phi_k) = \begin{pmatrix} D_1^* & D_2^* \\ D_3^* & D_4^* \end{pmatrix}$ and construct a new basis Υ for P^* by

$$\Upsilon = (\Upsilon_1, \Upsilon_2)^T = (\Upsilon^*, \Phi)^{-1}\Upsilon^*.$$

Then $(\Upsilon, \Phi) = I_2$. In addition, define $y_k := (\beta_k^1, \beta_k^2)$, where

$$\beta_k^1 = \begin{pmatrix} \cos\frac{k\pi}{l}x \\ 0 \end{pmatrix}, \quad \beta_k^2 = \begin{pmatrix} 0 \\ \cos\frac{k\pi}{l}x \end{pmatrix}.$$

We also define

$$c \cdot y_k = c_1\beta_k^1 + c_2\beta_k^2 \quad \text{for } c = (c_1, c_2)^T \in \mathbb{Y}_1.$$

$$(u, v) := \frac{1}{l\pi}\int_0^{l\pi} u_1\overline{v_1}dx + \frac{1}{l\pi}\int_0^{l\pi} u_2\overline{v_2}dx$$

for $u = (u_1, u_2)$, $v = (v_1, v_2)$, $u, v \in X$, and $(\varphi, y_0) = ((\varphi, y_0^1), (\varphi, y_0^2))^T$.

Rewrite (A.1) in the abstract form

$$\frac{dB_t(t)}{dt} = A_{\dot{\tau}}B_t + R(B_t, \varepsilon), \tag{A.10}$$

where

$$R(B_t, \varepsilon) = \begin{cases} 0, & \sigma \in [-1, 0), \\ Y(B_t, \varepsilon), & \sigma = 0. \end{cases} \tag{A.11}$$

The solution is

$$B_t = \Phi\begin{pmatrix} x_1 \\ x_2 \end{pmatrix} y_k + h(x_1, x_2, \varepsilon), \tag{A.12}$$

where

$$\begin{pmatrix} x_1 \\ x_2 \end{pmatrix} = (\Upsilon, < B_t, y_k >)$$

and

$$h(x_1, x_2, \varepsilon) \in P_S\mathscr{C}_1, \quad h(0, 0, 0) = 0, \quad Dh(0, 0, 0) = 0.$$

Then

$$B_t = \Phi\begin{pmatrix} x_1(t) \\ x_2(t) \end{pmatrix} y_k + h(x_1, x_2, 0). \tag{A.13}$$

Let $m = x_1 - ix_2$ and notice that $p_1 = \Phi_1 + i\Phi_2$. Then

$$\Phi\begin{pmatrix} x_1 \\ x_2 \end{pmatrix} y_k = (\Phi_1, \Phi_2)\begin{pmatrix} \frac{m+\overline{m}}{2} \\ \frac{i((m-\overline{m})}{2} \end{pmatrix} y_k = \frac{1}{2}(p_1 m + \overline{p_1 m})y_k$$

and

$$h(x_1, x_2, 0) = h\left(\frac{m + \overline{m}}{2}, \frac{i(m - \overline{m})}{2}, 0\right).$$

(A.13) becomes

$$\begin{aligned} B_t &= \frac{1}{2}(p_1 m + \overline{p_1 m})y_k + h\left(\frac{m+\overline{m}}{2}, \frac{i(m-\overline{m})}{2}, 0\right) \\ &= \frac{1}{2}(p_1 m + \overline{p_1 m})y_k + W(m, \overline{m}) \end{aligned} \tag{A.14}$$

where

$$W(m, \bar{m}) = h\left(\frac{m+\bar{m}}{2}, \frac{i(m-\bar{m})}{2}, 0\right)$$

and

$$\dot{m} = i\omega_k \dot{\tau} m + g(m, \bar{m}), \tag{A.15}$$

$$g(m, \bar{m}) = (\Upsilon_1(0) - i\Upsilon_2(0))\langle Y(B_t, 0), y_k\rangle. \tag{A.16}$$

Let

$$W(m, \bar{m}) = W_{20}\frac{m^2}{2} + W_{11} m\bar{m} + W_{02}\frac{\bar{m}^2}{2} + \cdots, \tag{A.17}$$

$$g(m, \bar{m}) = g_{20}\frac{m^2}{2} + g_{11} m\bar{m} + g_{02}\frac{\bar{m}^2}{2} + \cdots. \tag{A.18}$$

Then

$$u_t(0) = \frac{1}{2}(m + \bar{m})\cos\left(\frac{kx}{l}\right) + W_{20}^{(1)}(0)\frac{m^2}{2} + W_{11}^{(1)}(0) m\bar{m} + W_{02}^{(1)}(0)\frac{\bar{m}^2}{2} + \cdots,$$

$$v_t(0) = \frac{1}{2}(\delta + \bar{\delta}\bar{m})\cos\left(\frac{kx}{l}\right) + W_{20}^{(2)}(0)\frac{m^2}{2} + W_{11}^{(2)}(0) m\bar{m} + W_{02}^{(2)}(0)\frac{\bar{m}^2}{2} + \cdots,$$

$$u_t(-1) = \frac{1}{2}(ze^{-i\omega_k\dot{\tau}} + \bar{m}e^{i\omega_k\dot{\tau}})\cos\left(\frac{kx}{l}\right) + W_{20}^{(1)}(-1)\frac{m^2}{2} + W_{11}^{(1)}(-1) m\bar{m} + W_{02}^{(1)}(-1)\frac{\bar{m}^2}{2} + \cdots,$$

$$v_t(-1) = \frac{1}{2}(\delta z e^{-i\omega_k\dot{\tau}} + \bar{\delta}\bar{m}e^{i\omega_k\dot{\tau}})\cos\left(\frac{kx}{l}\right) + W_{20}^{(2)}(-1)\frac{m^2}{2} + W_{11}^{(2)}(-1) m\bar{m} + W_{02}^{(2)}(-1)\frac{\bar{m}^2}{2} + \cdots,$$

and

$$\begin{aligned} \bar{Y}_1(B_t, 0) &= \frac{1}{\dot{\tau}} Y_1 \\ &= \lambda_1 u_t^2(0) + \lambda_2 u_t(0)v_t(0) + \lambda_3 v_t^2(0) + \lambda_4 u_t^3(0) \\ &+ \lambda_5 u_t^2(0)v_t(0) + \lambda_6 u_t(0)v_t^2(0) + \lambda_7 v_t^3(0) + O(4). \end{aligned} \tag{A.19}$$

$$\begin{aligned} \bar{Y}_2(B_t, 0) &= \frac{1}{\dot{\tau}} Y_2 \\ &= \beta_1 u_t^2(-1) + \beta_2 u_t(-1)v_t(-1) + \beta_3 v_t^2(-1) + \beta_4 u_t^3(-1) \\ &+ \beta_5 u_t^2(-1)v_t(-1) + \beta_6 u_t(-1)v_t^2(-1) + \beta_7 v_t^3(-1) + O(4), \end{aligned} \tag{A.20}$$

where

$$\lambda_1 = \frac{2v_*^2\alpha_1}{(1+u_*v_*)^2} - 2, \qquad \lambda_2 = -\frac{2v_*\alpha_1}{(1+u_*v_*)^3}, \tag{A.21}$$

$$\lambda_3 = -\frac{2u_*\alpha_1}{(1+u_*v_*)^2}, \qquad \lambda_4 = -\frac{6v_*^4\alpha_1}{(1+u_*v_*)^4}, \tag{A.22}$$

$$\lambda_5 = \frac{6v_*^2\alpha_1}{(1+u_*v_*)^4}, \qquad \lambda_6 = \frac{2(-1+2u_*v_*)\alpha_1}{(1+u_*v_*)^4}, \tag{A.23}$$

$$\lambda_7 = \frac{6u_*^2\alpha_1}{(1+u_*v_*)^4}, \qquad \beta_1 = -\frac{2v_*^3\alpha_2}{(1+u_*v_*)^3}, \tag{A.24}$$

$$\beta_2 = \frac{2v_*\alpha_2}{(1+u_*v_*)^3}, \qquad \beta_3 = \frac{2u_*\alpha_2}{(1+u_*v_*)^3}, \tag{A.25}$$

$$\beta_4 = \frac{6v_*^4\alpha_2}{(1+u_*v_*)^4}, \qquad \beta_5 = -\frac{6v_*^2\alpha_2}{(1+u_*v_*)^4}, \tag{A.26}$$

$$\beta_6 = \frac{2(1-2u_*v_*)\alpha_2}{(1+u_*v_*)^4}, \qquad \beta_7 = -\frac{6u_*^2\alpha_2}{(1+u_*v_*)^4}. \tag{A.27}$$

Hence,

$$\begin{aligned}
\overline{Y}_1(B_t,0) &= \cos^2\left(\frac{kx}{l}\right)\left(\frac{m^2}{2}{}_{20} + m\overline{m}\chi_{11} + \frac{\overline{m}^2}{2}\overline{\chi}_{20}\right) \\
&\quad + \frac{m^2\overline{m}}{2}\left(\chi_1\cos\frac{kx}{l} + \chi_2\cos^3\frac{kx}{l}\right) + \cdots, \\
\overline{Y}_2(B_t,0) &= \cos^2\left(\frac{kx}{l}\right)\left(\frac{m^2}{2}\varsigma_{20} + m\overline{m}\varsigma_{11} + \frac{\overline{m}^2}{2}\overline{\varsigma}_{20}\right) \\
&\quad + \frac{m^2\overline{m}}{2}\left(\varsigma_1\cos\frac{kx}{l} + \varsigma_2\cos^3\frac{kx}{l}\right) + \cdots,
\end{aligned} \tag{A.28}$$

$$\begin{aligned}
\langle Y(B_t,0), y_k\rangle &= \dot{\tau}(\overline{Y}_1(B_t,0)y_k^1 + \overline{Y}_2(B_t,0)y_k^2) \\
&= \frac{m^2}{2}\dot{\tau}\begin{pmatrix}\chi_{20}\\ \varsigma_{20}\end{pmatrix}\Gamma + m\overline{m}\dot{\tau}\begin{pmatrix}\chi_{11}\\ \varsigma_{11}\end{pmatrix}\Gamma + \frac{\overline{m}^2}{2}\dot{\tau}\begin{pmatrix}\overline{\chi}_{20}\\ \overline{\varsigma}_{20}\end{pmatrix}\Gamma + \frac{m^2\overline{m}}{2}\dot{\tau}\begin{pmatrix}\kappa_1\\ \kappa_2\end{pmatrix} + \cdots
\end{aligned} \tag{A.29}$$

with

$$\begin{aligned}
\Gamma &= \frac{1}{l\pi}\int_0^{l\pi}\cos^3\left(\frac{kx}{l}\right)dx, \\
\kappa_1 &= \frac{\chi_1}{l\pi}\int_0^{l\pi}\cos^2\left(\frac{kx}{l}\right)dx + \frac{\chi_2}{l\pi}\int_0^{l\pi}\cos^4\left(\frac{kx}{l}\right)dx, \\
\kappa_2 &= \frac{\varsigma_1}{l\pi}\int_0^{l\pi}\cos^2\left(\frac{kx}{l}\right)dx + \frac{\varsigma_2}{l\pi}\int_0^{l\pi}\cos^4\left(\frac{kx}{l}\right)dx,
\end{aligned}$$

and

$$\chi_{20} = \frac{1}{2}(\lambda_1 + \delta(\lambda_2 + \lambda_3\delta))\,\chi_{11} = \frac{1}{4}(2\alpha_1 + 2\alpha_3\overline{\delta}\delta + \alpha_2(\overline{\delta} + \delta)),$$

$$\begin{aligned}
\chi_1 &= W_{11}^{(1)}(0)(2\lambda_1+\lambda_2\delta)+W_{11}^{(2)}(0)(\lambda_2+2\lambda_3\delta)\\
&\quad+W_{20}^{(1)}(0)\left(\lambda_1+\frac{\lambda_2\overline{\delta}}{2}\right)+W_{20}^{(2)}(0)\left(\lambda_3\overline{\delta}+\frac{\lambda_2}{2}\right),\\
\chi_2 &= \frac{1}{4}(3\lambda_4+\lambda_5(\overline{\delta}+2\delta)+\delta(2\lambda_6\overline{\delta}+\lambda_6\delta+3\lambda_7\overline{\delta}\delta)),\\
\varsigma_{20} &= \frac{1}{2}e^{-2i\omega_k}(\beta_1+\delta(\beta_2+(e^{2i\omega_k}\beta_3)\delta)),
\end{aligned}$$

$$\begin{aligned}
\varsigma_{11} &= \frac{1}{4}(2\beta_1+2\beta_3)\overline{\delta}\delta+\beta_2(\overline{\delta}+\delta)),\\
\varsigma_1 &= e^{-i\overline{\omega}_k}W_{11}^1(-1)(2\beta_1+\beta_2\delta)\\
&\quad+e^{-i\overline{\omega}_k}W_{11}^2(-1)(\beta_2+2\beta_3\delta)+\frac{1}{2}e^{i\overline{\omega}_k}W_{20}^1(-1)(2\beta_1+\beta_2\overline{\delta})\\
&\quad+\frac{1}{2}e^{i\overline{\omega}_k}W_{20}^2(-1)(\beta_2+2\beta_3\overline{\delta}),\\
\varsigma_2 &= \frac{1}{4}e^{-i\overline{\omega}_k}(3\beta_4+\beta_5(\overline{\delta}+2\delta)+3\beta_7\overline{\delta}\delta^2+\beta_6(2\overline{\delta}+\delta))).
\end{aligned}$$

Denote

$$\gamma_1(0)-i\gamma_2(0):=(\gamma_1\ \gamma_2).$$

Notice that

$$\frac{1}{l\pi}\int_0^{l\pi}\cos^3\frac{kx}{l}dx=0,\quad k=1,2,3,\cdots.$$

We have

$$\begin{aligned}
&(\gamma_1(0)-i\gamma_2(0))\langle Y(B_t,0),y_k\rangle\\
&=\frac{m^2}{2}(\gamma_1\chi_{20}+\gamma_2\varsigma_{20})\Gamma\dot{\tau}+m\overline{m}(\gamma_1\chi_{11}+\gamma_2\varsigma_{11})\Gamma\dot{\tau}+\frac{\overline{m}^2}{2}(\gamma_1\overline{\chi}_{20}+\gamma_2\overline{\varsigma}_{20})\Gamma\dot{\tau}\\
&+\frac{m^2\overline{m}}{2}\dot{\tau}[\gamma_1\kappa_1+\gamma_2\kappa_2]+\cdots.
\end{aligned}\tag{A.30}$$

Then by (A.16), (A.18), and (A.30) we have

$$g_{20}=\gamma_1\dot{\tau}\chi_{20}+\gamma_2\dot{\tau}\varsigma_{20},\quad g_{11}=\gamma_1\dot{\tau}\chi_{11}+\gamma_2\dot{\tau}\varsigma_{11},\quad g_{02}=\gamma_1\dot{\tau}\overline{\chi}_{20}+\gamma_2\dot{\tau}\overline{\varsigma}_{20},\tag{A.31}$$

and for $k\in\mathbb{N}_0$, we have $g_{21}=\dot{\tau}(\gamma_1\kappa_1+\gamma_2\kappa_2)$.
From [20] we have

$$\dot{W}(m,\overline{m})=W_{20}m\dot{z}+W_{11}\dot{z}\overline{m}+W_{11}m\dot{\overline{m}}+W_{02}\dot{\overline{m}}\overline{m}+\cdots,\tag{A.32}$$

$$A_{\dot{\tau}}\tilde{W}(m,\overline{m})=A_{\dot{\tau}}W_{20}\frac{m^2}{2}+A_{\dot{\tau}}W_{11}m\overline{m}+A_{\dot{\tau}}W_{02}\frac{\overline{m}^2}{2}+\cdots,\tag{A.33}$$

and

$$\dot{W}(m,\overline{m}) = A_{\dot{\tau}}W + H(m,\overline{m}), \tag{A.34}$$

where

$$\begin{aligned} H(m,\overline{m}) &= H_{20}\frac{m^2}{2} + W_{11}m\overline{m} + H_{02}\frac{\overline{m}^2}{2} + \cdots \\ &= \chi_0 Y(B_t,0) - \Phi(\gamma, \langle \chi_0 Y(B_t,0), y_k\rangle \cdot y_k). \end{aligned} \tag{A.35}$$

Hence, we obtain

$$(2i\omega_k\dot{\tau} - A_{\dot{\tau}})W_{20} = H_{20}, \quad -A_{\dot{\tau}}W_{11} = H_{11}, \quad (-2i\omega_k\dot{\tau} - A_{\dot{\tau}})W_{02} = H_{02}, \tag{A.36}$$

$$W_{20} = (2i\omega_k\dot{\tau} - A_{\dot{\tau}})^{-1}H_{20}, \quad W_{11} = -A_{\dot{\tau}}^{-1}H_{11}, \quad W_{02} = (-2i\omega_k\dot{\tau} - A_{\dot{\tau}})^{-1}H_{02}. \tag{A.37}$$

$$\begin{aligned} H(m,\overline{m}) &= -\Phi(0)\gamma(0)\langle Y(B_t,0), y_k\rangle \cdot y_k \\ &= -\left(\frac{p_1(\sigma)+p_2(\sigma)}{2}, \frac{p_1(\sigma)-p_2(\sigma)}{2i}\right)\begin{pmatrix}\Phi_1(0)\\ \Phi_2(0)\end{pmatrix}\langle Y(B_t,0), y_k\rangle \cdot y_k \\ &= -\frac{1}{2}[p_1(\sigma)(\Phi_1(0) - i\Phi_2(0)) + p_2(\sigma)(\Phi_1(0) + i\Phi_2(0))]\langle Y(B_t,0), y_k\rangle \cdot y_k \\ &= -\frac{1}{2}\Bigg[(p_1(\sigma)g_{20} + p_2(\sigma)\overline{g}_{02})\frac{m^2}{2} + (p_1(\sigma)g_{11} + p_2(\sigma)\overline{g}_{11})m\overline{m} \\ &\quad + (p_1(\sigma)g_{02} + p_2(\sigma)\overline{g}_{20})\frac{\overline{m}^2}{2}\Bigg] + \cdots . \end{aligned}$$

Therefore,

$$\begin{aligned} H_{20}(\sigma) &= \begin{cases} 0, & k \in \mathbb{N}, \\ -\frac{1}{2}(p_1(\sigma)g_{20} + p_2(\sigma)\overline{g}_{02}) \cdot y_0, & k = 0, \end{cases} \\ H_{11}(\sigma) &= \begin{cases} 0, & k \in \mathbb{N}, \\ -\frac{1}{2}(p_1(\sigma)g_{11} + p_2(\sigma)\overline{g}_{11}) \cdot y_0, & k = 0, \end{cases} \\ H_{02}(\sigma) &= \begin{cases} 0, & k \in \mathbb{N}, \\ -\frac{1}{2}(p_1(\sigma)g_{02} + p_2(\sigma)\overline{g}_{20}) \cdot y_0, & k = 0, \end{cases} \end{aligned}$$

and

$$H(m,\overline{m})(0) = Y(B_t,0) - \Phi(\gamma, \langle Y(B_t,0), y_k\rangle) \cdot y_k,$$

where

$$H_{20}(0) = \begin{cases} \dot{\tau}\begin{pmatrix}\chi_{20}\\ \varsigma_{20}\end{pmatrix}\cos^2\left(\frac{kx}{l}\right), & k \in \mathbb{N}, \\ \dot{\tau}\begin{pmatrix}\chi_{20}\\ \varsigma_{20}\end{pmatrix} - \frac{1}{2}(p_1(0)g_{20} + p_2(0)\overline{g}_{02}) \cdot y_0, & k = 0, \end{cases}$$

$$H_{11}(0) = \begin{cases} \dot{\tau}\begin{pmatrix}\chi_{11}\\ \varsigma_{11}\end{pmatrix}\cos^2\left(\frac{kx}{l}\right), & k \in \mathbb{N}, \\ \dot{\tau}\begin{pmatrix}\chi_{11}\\ \varsigma_{11}\end{pmatrix} - \frac{1}{2}(p_1(0)g_{11} + p_2(0)\overline{g}_{11})\cdot y_0, & k = 0. \end{cases}$$

We have

$$\dot{W}_{20} = A_{\dot{\tau}}W_{20} = 2i\omega_k\dot{\tau}W_{20} + \frac{1}{2}(p_1(\sigma)g_{20} + p_2(\sigma)\overline{g}_{02})\cdot y_k, \quad -1 \le \sigma < 0.$$

That is,

$$W_{20}(\sigma) = \frac{i}{2i\omega_k\dot{\tau}}\left(g_{20}p_1(\sigma) + \frac{\overline{g}_{02}}{3}p_2(\sigma)\right)\cdot y_k + E_1 e^{2i\omega_k\dot{\tau}\sigma},$$

where

$$E_1 = \begin{cases} W_{20}(0), & k = 1, 2, 3, \cdots, \\ W_{20}(0) - \frac{i}{2\omega_k\dot{\tau}}(g_{20}p_1(\sigma) + \frac{\overline{g}_{02}}{3}p_2(\sigma))\cdot y_0, & k = 0. \end{cases}$$

We have that

$$\begin{aligned} &-(g_{20}p_1(0) + \frac{\overline{g}_{02}}{3}p_2(0))\cdot y_0 + 2i\omega_k\dot{\tau}E_1 - A_{\dot{\tau}}\left(\frac{i}{2\omega_k\dot{\tau}}\left(g_{20}p_1(0) + \frac{\overline{g}_{02}}{3}p_2(0)\right)\cdot y_0\right) \\ &- A_{\dot{\tau}}E_1 - L_{\dot{\tau}}\left(\frac{i}{2\omega_k\dot{\tau}}\left(g_{20}p_1(0) + \frac{\overline{g}_{02}}{3}p_2(0)\right)\cdot y_k + E_1 e^{2i\omega_k\dot{\tau}\sigma}\right) \\ &= \dot{\tau}\begin{pmatrix}\chi_{20}\\ \varsigma_{20}\end{pmatrix} - \frac{1}{2}(p_1(0)g_{20} + p_2(0)\overline{g}_{02})\cdot y_0. \end{aligned}$$

As

$$\begin{aligned} &A_{\dot{\tau}}p_1(0) + L_{\dot{\tau}}(p_1\cdot y_0) = i\omega_0 p_1(0)\cdot y_0, \\ &A_{\dot{\tau}}p_2(0) + L_{\dot{\tau}}(p_2\cdot y_0) = -i\omega_0 p_2(0)\cdot y_0, \\ &2i\omega_0 E_1 - A_{\dot{\tau}}E_1 - L_{\dot{\tau}}E_1 e^{2i\omega_0\dot{\tau}} = \dot{\tau}\begin{pmatrix}\chi_{20}\\ \varsigma_{20}\end{pmatrix}\cos^2\left(\frac{kx}{l}\right), \quad k \in \mathbb{N}_0. \end{aligned}$$

That is,

$$E_1 = \dot{\tau}E\begin{pmatrix}\chi_{20}\\ \varsigma_{20}\end{pmatrix}\cos^2\left(\frac{kx}{l}\right),$$

$$E = \begin{pmatrix} 2i\omega_k\dot{\tau} - a_1 + d_1\frac{k^2}{l^2} & -a_2 \\ -b_1 e^{-2i\omega_k\dot{\tau}} & 2i\omega_k\dot{\tau} - b_2 e^{-2i\omega_0\dot{\tau}} + \gamma + h_2 + d_2\frac{k^2}{l^2} \end{pmatrix}^{-1},$$

$$-\dot{W}_{11} = \frac{i}{2\omega_k\dot{\tau}}(p_1(\sigma)g_{11} + p_2(\sigma)\overline{g}_{11})\cdot y_k, \quad -1 \le \sigma < 0,$$

$$W_{11}(\sigma) = \frac{i}{2i\omega_k\dot{\tau}}(p_1(\sigma)\overline{g}_{11} - p_1(\sigma)g_{11}) + E_2,$$

$$E_2 = \dot{\tau}E^* \begin{pmatrix} \chi_{11} \\ \varsigma_{11} \end{pmatrix} \cos^2\left(\frac{kx}{l}\right),$$

$$E^* = \begin{pmatrix} -a_1 + d_1\frac{k^2}{l^2} & -ra_2 \\ -b_1 & -b_2 + \gamma + h_2 + d_2\frac{k^2}{l^2} \end{pmatrix}^{-1}.$$